International Journal of Scientific & Engineering Research, Volume 6, Issue 6, June-2015
ISSN 2229-5518

A New Robust Fuzzy Sliding Mode Control of Robot Manipulator in the Task Space in Presence of Uncertainties

Mohammad Veysi

Abstract— This paper presents a new method to control of robot manipulator in task space. In the proposed control method, a combination of feedback linearization, sliding mode control and first-order TSK fuzzy system has been utilized. In this method, the bounds of structural and non-structural uncertainties by using feedback linearization method are reduced and to overcome the remaining uncertainties, sliding mode control is deployed. The presence of sliding mode control triggers the adverse phenomenon of chattering in controlling the robot manipulator in task space. Finally, to prevent the occurrence of chattering and to precise tracking of the desired trajectory in task space with minimal position tracking error, TSK fuzzy system is utilized in the control input. To examine the performance of the proposed control, a two-degree-of-freedom manipulator is used as a case study. The results of simulation demonstrated the favorable performance of the proposed method.

Index Terms— Robot manipulator, Task space, Fuzzy sliding mode control, Feedback linearization, Uncertainty, Tracking position error, Chattering.

1 Introduction

THE dynamics of robot manipulators are highly nonlinear with large couplings and uncertainties in model. Therefore, challenge in robot control to dominate uncertainties, nonlinearities and couplings from various aspects in the robust control method as reviewed in [1, 2]. According to sliding mode control's capability in facing model uncertainties and system disturbances, it has attracted considerable attention in controlling industrial manipulators [3, 4]. The robust control provides stability under uncertainties with a tradeoff between tracking performance and bounds of uncertainties. This control approach was extensively presented in the joint space to execute position control [5] while controlling a robot in the task space is still a control problem. Actually, for tracking application in the task space, the industrial robot follow a desired trajectory in the joint space recorded by "teach and play back" technique. Feedbacks from the joint positions are given to the control system. Therefore, the control system cannot realize directly the position error of the end effector. However, industrial robots can perform desired tasks. Because industrial robots are produced in a high quality with a good repeatability, precision, and resolution. But, a high cost should be expended to achieve the mentioned specifications. In contrast, the use of inferior robots increases the uncertainties. The performance of robot can be improved by improving the control system. A robot should show a reasonable position tolerance in the operating range. However, the robot cannot achieve to a precise position in the workspace without feedback from the end effector position. Therefore, despite many efforts, the robust joint space control [6-12] cannot be able to provide a perfect performance in the task space under uncertain kinematics.

• *Department of Electrical Engineering, Shahid Sattari Aeronautical University of Science and Technology, Tehran, Iran.*
E-mail: veysi@ssau.ac.ir

However, in sliding mode control method, control input has discontinuity in implementation step, so called control chattering [13, 14]. This chattering leads to activation of robot manipulator's dynamic modes which in turn reduces the efficiency of control input [1, 3, 4]. So far several techniques for eliminating control chattering in sliding mode control have been proposed, such as methods: terminal sliding mode control [15, 16], integral sliding mode control [17-20], dynamic sliding mode control [21, 22], higher degree sliding control mode [23-25], sliding mode control by utilizing shifted and rotational sliding surfaces [26, 27], designing sliding surfaces based on linear matrices for systems with time delay and uncertainty [19, 28-30]. Although the aforementioned methods for eliminating control chattering contain several advantages, they have disadvantages which cause a number of problems in the operations of the control system. Some of these bugs are as follows: In most of these methods, the reduction in control chattering has led to an increase in tracking error. The presence of integral term in the design of sliding surface will cause a phenomenon named "integrator wind-up" and, as a result, it leads to the saturation of controllers and actuators as well as system instability. Resolutions to this phenomenon significantly increase the calculations content. Complex calculations cause time delay in process of control system and actuators and eliminate real-time control and occasionally challenges control system stability.

In this paper, in order to avoid challenges of the robot manipulator control in joint space and to precise tracking of the desired trajectory in task space, feedbacks from the end effector position are given to the control system. In fact, according to the dynamic equation of robot in task space, robust controller is designed. As well as, to improve the capabilities of sliding mode controller, in controlling position tracking error, encountering adverse phenomenon of chattering in control input and to avoid problems of the aforementioned methods in the previous paragraph, the first-order fuzzy TSK system will be utilized.

This paper is organized as follows: Section 2 introduces dynamic equation of a robot manipulator in joint space. In section 3, to design the proposed control, the equations of the robot manipulator are transferred to the task space. In section 4, based on the dynamic equations and using the feedback linearization method, a sliding mode controller is designed to control robot manipulator in task space. Mathematical proof shows that the closed-loop system with this controller has a global asymptotic stability. Next, to eliminate the adverse phenomenon of chattering in the control input, the technique of a boundary layer creation around the zero sliding surface is used. In this technique, though control law is free of chattering, the precision in the tracking of robot manipulator position has decreased and the controller is encountered with tracking error. Nevertheless, in most industrial applications, precise tracking of the desired trajectory by means of a robot is considerable. In section 5, after expressing the deficiencies of the proposed method, first order TSK fuzzy system is employed in order to eliminate the chattering phenomena and guarantees tracking the desired trajectory by means of robot manipulator in task apace. In section 6, to exhibit the performance of the proposed control, simulations in three steps are implemented on a two-degree-of-freedom robot manipulator. The results of simulation indicate the performance of the proposed control. Ultimately, section 7 describes the conclusions.

2 DYNAMIC EQUATIONS OF A ROBOT MANIPULATOR IN JOINT SPACE

Dynamic equation of a robot manipulator in joint space is a nonlinear, multi-input, multi-output and second order differential equation which is expressed as follows [31]:

$$M(q)\ddot{q} + V(q,\dot{q})\dot{q} + G(q) + T_d = u \,, \tag{1}$$

In which $\mathrm{M(q)} \in \mathrm{R}^{n\times n}$ represents the inertia matrix, $\mathrm{V}(q,\dot{q}) \in \mathrm{R}^{n\times n}$ is a matrix including sections related to Coriolis and centrifugal forces, $\mathrm{G(q)} \in \mathrm{R}^n$ stands for the gravitation vector, $\mathrm{T_d} \in \mathrm{R}^n$ is a vector including disturbances or un-modeled dynamics, $\mathrm{q(t)} \in \mathrm{R}^n$ is designated as the vector of joint positions, $\dot{q}(t) \in \mathrm{R}^n$ is assigned as the vector of joint velocities, $\ddot{q}(t) \in \mathrm{R}^n$ is the vector of joint accelerations, and $u \in \mathrm{R}^n$ is the vector of robot manipulator input torque.
To simplify equation (1), the following equation is defined:

$$\mathrm{H}(q,\dot{q}) = \mathrm{V}(q,\dot{q})\dot{q} + \mathrm{G}(q) + \mathrm{T_d} \,, \tag{2}$$

By substituting (2) in (1) we obtain:

$$\mathrm{M}(q)\ddot{q} + \mathrm{H}(q,\dot{q}) = u \,, \tag{3}$$

Relation (1) has the following specifications:

Specifications 1: inertia matrix M(q) is symmetric and positive-definite.

3 DYNAMIC EQUATIONS OF A ROBOT MANIPULATOR IN TASK SPACE

To design controller in task space, the dynamic equation of robot manipulator in task space is used. For this purpose, equation (3) can be simplified as follows [32]:

$$\ddot{q} = \mathrm{M}^{-1}(q)\big(u - \mathrm{H}(q,\dot{q})\big) \,, \tag{4}$$

To obtain the velocity of end-effector in task space, the following equation is used [31]:

$$\dot{\mathrm{X}} = \mathrm{J}(q)\dot{q} \,, \tag{5}$$

In which $\mathrm{J}(q) \in \mathrm{R}^{n\times n}$ represents the Jacobian matrix, $\dot{q}(t) \in \mathrm{R}^n$ is the vector of joint velocities, and $\dot{\mathrm{X}}(t) \in \mathrm{R}^n$ is the vector of velocity in task space. Differentiating with respect to time in equation (5), we obtain:

$$\ddot{\mathrm{X}} = \mathrm{J}(q)\ddot{q} + \dot{\mathrm{J}}(q)\dot{q} \,, \tag{6}$$

Smoothness of trajectory is condition of existence $\dot{\mathrm{J}}(q)$. Assuming that the task space trajectory is free from singularities, substituting equation (4) in (6), we obtain:

$$\ddot{\mathrm{X}} = \mathrm{J}(q)\mathrm{M}^{-1}(q)(u - \mathrm{H}(q,\dot{q})) + \dot{\mathrm{J}}(q)\dot{q} \,, \tag{7}$$

Equation (7) is rewritten as:

$$\mathrm{M}(q)\mathrm{J}^{-1}(q)\ddot{\mathrm{X}} + \mathrm{H}(q,\dot{q}) - \mathrm{M}(q)\mathrm{J}^{-1}(q)\dot{\mathrm{J}}(q)\dot{q} = u \,, \tag{8}$$

$\mathrm{J}^{-1}(q)$ is inverse Jacobian matrix.

Assumption 1: We assume that the robot is operating in a finite task space such that the Jacobian matrix is full rank.
For transmission of torque space to force space, the following equation can be used [31]:

$$u = \mathrm{J}^{T}(q)\mathrm{F}(t) \,, \tag{9}$$

Where $\mathrm{J}^{T}(q)$ is Jacobian matrix transpose and $\mathrm{F}(t) \in \mathrm{R}^n$ is a force vector acting on the end-effector of the robot. Equation (9) in (8) is substituted and arranged as:

$$\mathrm{J}^{-T}(q)\mathrm{M}(q)\mathrm{J}^{-1}(q)\ddot{\mathrm{X}} + \mathrm{J}^{-T}(q)\mathrm{H}(q,\dot{q}) - \mathrm{J}^{-T}(q)\mathrm{M}(q)\mathrm{J}^{-1}(q)\dot{\mathrm{J}}(q)\dot{q} = \mathrm{F}(t) \,, \tag{10}$$

According to equations (2) and (10), the following equations are defined as:

$$\begin{cases} \mathrm{M_x}(q) = \mathrm{J}^{-T}(q)\mathrm{M}(q)\mathrm{J}^{-1}(q) \\ \mathrm{v_x}(q,\dot{q}) = \mathrm{J}^{-T}(q)\big(\mathrm{v}(q,\dot{q}) - \mathrm{M}(q)\mathrm{J}^{-1}(q)\dot{\mathrm{J}}(q)\dot{q}\big) \\ \mathrm{G_x}(q) = \mathrm{J}^{-T}(q)\mathrm{G}(q) \,, \end{cases} \tag{11}$$

In the above equations, analogous to the joint space quantities, $\mathrm{M_x}(q) \in \mathrm{R}^{n\times n}$ is the Cartesian mass matrix, $\mathrm{v_x}(q,\dot{q}) \in \mathrm{R}^{n\times n}$ is a vector of velocity terms in Cartesian space and $\mathrm{G_x}(q) \in \mathrm{R}^n$ is a vector of gravity terms in Cartesian space. $\mathrm{H_x}(q,\dot{q})$ is defined as:

$$\mathrm{H}_x(q,\dot{q}) = \mathrm{V_x}(q,\dot{q})\dot{q} + \mathrm{G_x}(q) + \mathrm{T}_{dX} \,, \tag{12}$$

According to the equations (10) and (12), the dynamic equations of robot manipulator in task space can be obtained as follows:

$$\mathrm{M}_x(q)\ddot{\mathrm{X}} + \mathrm{H_x}(q,\dot{q}) = \mathrm{F}(t) \,, \tag{13}$$

In equations (12) and (13), $X(t) \in \mathrm{R}^n$ is an appropriate Cartesian vector representing position and orientation of the end-effector [33], $\dot{X}(t) \in \mathrm{R}^n$ is the velocity vector of end-effector in Cartesian space, $\ddot{X}(t) \in \mathrm{R}^n$ is the vector of end-effector acceleration in Cartesian space and $T_{dX} \in \mathrm{R}^n$ is a vector including disturbances or un-modeled dynamics in Cartesian space.

Definition 1: Sylvester's law of inertia: If $A \in R^{n\times n}$ is a symmetric square matrix and $C \in R^{n\times n}$ is non-singular matrix, then the number of positive, negative and zero eigenvalues of matrix A and matrix C^TAC are the same, where C^T is the transpose of C [34].

According to the equation $M_x(q) = J^{-T}(q)M(q)J^{-1}(q)$ and due to the non-singularity of $J^{-1}(q)$ and in view of the specifications 1 expressed in Section 2, using Sylvester's law of inertia, the specifications 2 can be deduced.

Specifications 2: Cartesian mass matrix $M_x(q)$ is a positive-definite matrix.

4 DESIGN OF SLIDING MODE CONTROLLER FOR ROBOT MANIPULATOR IN TASK SPACE

To design sliding mode control, sliding surface vector is defined as [13]:

$$S = \left({}^{d}\!/_{dt} + \lambda\right)^{n-1} e\,, \tag{14}$$

In equation (14), $e = X - X_d$ represents the tracking error vector in which $X = [x_1\ x_2\ \dots\ x_n]^T$ is the vector of end-effector position and $X_d = [x_{1d}\ x_{2d} \dots x_{nd}]^T$ is the vector of desired trajectory in Cartesian space and $\lambda = diag[\lambda_1, \lambda_2, \dots, \lambda_n]$ is a diagonal matrix in which $\lambda_1, \lambda_2, \dots, \lambda_n$ are constant and positive coefficients. Generally, to design sliding mode controller, the variable $x_r^{(n-1)}$ is defined as:

$$x_r^{(n-1)} = x^{(n-1)} - s\,, \tag{15}$$

Since the robot manipulator is expressed by the second order differential equation, equation (15) with $n = 2$ is determined as:

$$\dot{x}_r = \dot{x} - s\,, \tag{16}$$

Differentiating equation (16), we obtain:

$$\ddot{x}_r = \ddot{x} - \dot{s}\,, \tag{17}$$

Point 1: Since x, $\dot{x}$, $\ddot{x}$ and S are $n \times 1$ vectors, thus $\dot{x}_r$ and $\ddot{x}_r$ are $n \times 1$ vectors.

To design sliding mode controller, with respect to equations (16) and (17), equation (13) is changed into:

$$M_x(q)\ddot{x}_r + M_x(q)\dot{s} + H_x(q,\dot{q}) = F(t)\,, \tag{18}$$

Next, the control law is proposed as:

$$F(t) = \hat{F}(t) - Ksgn(s) - As\,, \tag{19}$$

In which sgn(s) is the sign function and $\hat{F}(t)$ is selected as:

$$\hat{F}(t) = \hat{M}_x(q)\ddot{x}_r + \hat{H}_x(q,\dot{q})\,, \tag{20}$$

In equations (19) and (20), $\hat{M}_x(q)$ and $\hat{H}_x(q,\dot{q})$ are estimations of $M_x(q)$ and $H_x(q,\dot{q})$ respectively and $K = diag[k_1, k_2, \dots, k_n]$ is a positive-definite diagonal matrix and $A = \begin{bmatrix} A_{11} & \cdots & A_{1n} \\ \vdots & \ddots & \vdots \\ A_{n1} & \cdots & A_{nn} \end{bmatrix}$ is a positive-definite matrix. Substituting equations (19) and (20) in (18), we obtain:

$$M_x(q)\ddot{x}_r + M_x(q)\dot{s} + H_x(q,\dot{q}) = \hat{M}_x(q)\ddot{x}_r + \hat{H}_x(q,\dot{q}) - Ksgn(s) - As\,, \tag{21}$$

Equation (21) is simplified as:

$$M_x(q)\dot{s} = \left(\hat{M}_x(q) - M_x(q)\right)\ddot{x}_r + \left(\hat{H}_x(q,\dot{q}) - H_x(q,\dot{q})\right) - As - Ksgn(s)\,, \tag{22}$$

For the sake of simplicity of the aforementioned equations, $\Delta M_x(q) = \hat{M}_x(q) - M_x(q)$, $\Delta H_x(q,\dot{q}) = \hat{H}_x(q,\dot{q}) - H_x(q,\dot{q})$ and $\Delta f = \Delta M_x(q)\ddot{x}_r + \Delta H_x(q,\dot{q})$ are defined and equation (22) is simplified as:

$$M_x(q)\dot{s} = \Delta M_x(q)\ddot{x}_r + \Delta H_x(q,\dot{q}) - As - Ksgn(s) = \Delta f - As - Ksgn(s)\,, \tag{23}$$

Point 2: $\Delta f \in R^n$ is a vector including all parametric, non-structural uncertainties as well as un-modeled dynamics.

4.1 Proof of closed-loop system stability

To prove closed-loop system stability of equation (22) with respect to the dynamic features of robot manipulator as mentioned in section 3, Lyapunov function candidate is proposed as:

$$V(s) = \tfrac{1}{2} s^T M_x(q) s\,, \tag{24}$$

Differentiating with respect to time in equation (24), we obtain:

$$\dot{V}(s) = s^T M_x(q)\dot{s} + \tfrac{1}{2} s^T \dot{M}_x(q) s\,, \tag{25}$$

Differentiating with respect to time of all entries of matrix $M_x(q)$ and $\dot{M}_x(q)$ is defined as:

$$\dot{M}_x(q) = \begin{bmatrix} D_{11} & \cdots & D_{1n} \\ \vdots & \ddots & \vdots \\ D_{n1} & \cdots & D_{nn} \end{bmatrix}, \tag{26}$$

With respect to equations (23) and (26), equation (25) is rewritten, and to understand it easier, the equations are presented in matrix form [32]:

$$\dot{V}(s) = [s_1\ s_2\ \dots\ s_n] \times \left(\begin{bmatrix} \Delta f_1 \\ \Delta f_2 \\ \vdots \\ \Delta f_n \end{bmatrix} - \begin{bmatrix} A_{11} & \cdots & A_{1n} \\ \vdots & \ddots & \vdots \\ A_{n1} & \cdots & A_{nn} \end{bmatrix} \begin{bmatrix} s_1 \\ s_2 \\ \vdots \\ s_n \end{bmatrix} - \begin{bmatrix} k_1 & 0 & 0 \\ 0 & \ddots & 0 \\ 0 & 0 & k_n \end{bmatrix} \begin{bmatrix} sgn(s_1) \\ sgn(s_2) \\ \vdots \\ sgn(s_n) \end{bmatrix} \right) + \tfrac{1}{2}[s_1\ s_2\ \dots\ s_n] \begin{bmatrix} D_{11} & \cdots & D_{1n} \\ \vdots & \ddots & \vdots \\ D_{n1} & \cdots & D_{nn} \end{bmatrix} \begin{bmatrix} s_1 \\ s_2 \\ \vdots \\ s_n \end{bmatrix}, \tag{27}$$

After simplifying equation (27), in three steps, the following equations can be concluded:

$$\dot{V}(s) = [s_1\ s_2\ \dots\ s_n] \times \left(\begin{bmatrix} \Delta f_1 \\ \Delta f_2 \\ \vdots \\ \Delta f_n \end{bmatrix} - \begin{bmatrix} \sum_{i=1}^{n} s_i A_{1i} \\ \sum_{i=1}^{n} s_i A_{2i} \\ \vdots \\ \sum_{i=1}^{n} s_i A_{ni} \end{bmatrix} - \begin{bmatrix} k_1 sgn(s_1) \\ k_2 sgn(s_2) \\ \vdots \\ k_n sgn(s_n) \end{bmatrix} \right) + \frac{1}{2} \left[\sum_{i=1}^{n} s_i D_{i1}\ \sum_{i=1}^{n} s_i D_{i2}\ \dots\ \sum_{i=1}^{n} s_i D_{in} \right] \begin{bmatrix} s_1 \\ s_2 \\ \vdots \\ s_n \end{bmatrix}, \tag{28}$$

$$\dot{V}(s) = [s_1\ s_2\ \dots\ s_n] \times \begin{bmatrix} \Delta f_1 - \sum_{i=1}^{n} s_i A_{1i} - k_1 sgn(s_1) \\ \Delta f_2 - \sum_{i=1}^{n} s_i A_{2i} - k_2 sgn(s_2) \\ \vdots \\ \Delta f_n - \sum_{i=1}^{n} s_i A_{ni} - k_n sgn(s_n) \end{bmatrix} + \frac{1}{2} \left(\sum_{i=1}^{n} s_i s_1 D_{i1} + \sum_{i=1}^{n} s_i s_2 D_{i2} + \dots + \sum_{i=1}^{n} s_i s_n D_{in} \right), \tag{29}$$

$$\dot{V}(s) = \sum_{i=1}^{n} (s_i(\Delta f_i - k_i sgn(s_i))) - \sum_{i=1}^{n} \sum_{j=1}^{n} s_i s_j A_{ij} + \frac{1}{2} \sum_{i=1}^{n} \sum_{j=1}^{n} s_i s_j D_{ij}, \tag{30}$$

In equation (30), s_i is ith entries of sliding surface vector S , Δf_i is ith entries of vector Δf, K_i is ith entries of the main diameter of matrix k, A_{ij} is entries in ith rows and jth columns of matrix A; in addition, D_{ij} is entries in ith rows and jth columns of matrix $\dot{M}_x(q)$. To prove closed-loop system stability, equation (30) must be less than zero, that is:

$$\dot{V}(s) = \sum_{i=1}^{n} (s_i(\Delta f_i - k_i sgn(s_i))) - \sum_{i=1}^{n} \sum_{j=1}^{n} s_i s_j A_{ij} + \frac{1}{2} \sum_{i=1}^{n} \sum_{j=1}^{n} s_i s_j D_{ij} < 0, \tag{31}$$

The aforementioned equation is satisfied if:

$$K_i > \|\Delta f_i\|, \tag{32}$$

$$\|A_{ij}\| > \left\| \frac{D_{ij}}{2} \right\|. \tag{33}$$

Thus by selecting appropriate K which satisfies equation (32) and also by selecting appropriate A which satisfies equation (33), closed-loop system will possess the global asymptotic stability.

4.2 Modification of proposed control

Although robot manipulator with the proposed controller will have global asymptotic stability, control input will have chattering which can activate the dynamic modes of robot manipulator. Thus to avoid such an adverse phenomenon, control law is modified as [13]:

$$\mathrm{F(t)} = \hat{\mathrm{F}}(\mathrm{t}) - Ksat(^{s}/_{\phi}) - As, \tag{34}$$

In the aforementioned equation, by choosing the proper ϕ (boundary layer thickness), we can eliminate chattering at control input; however, we will have no control on the tracking error of robot manipulator position. As a matter of fact, by selecting various ϕ , one of the following conditions will occur in the controller:

1.By choosing large ϕ, chattering in control input would be eliminated and the error in robot manipulator tracking position will increase.

2.By choosing small ϕ, the accuracy in tracking position robot manipulator will improve, but unfortunately, the chattering phenomenon will occur.

Nevertheless, in most applications of robot manipulator such as assembling, eliminating control input chattering as well as accuracy in tracking robot manipulator position is of significant importance. Therefore, to improve the capabilities of this controller, in controlling position tracking error and encountering unfavorable phenomenon of chattering in control input, we will utilize the first-order fuzzy TSK system.

5 DESIGN OF FUZZY SLIDING MODE CONTROLLER FOR ROBOT MANIPULATOR IN TASK SPACE

A first-order fuzzy TSK system is delineated by fuzzy if-then rules which show the relations between inputs and outputs. Generally, first-order fuzzy TSK control system rules are defined as:

$$\begin{aligned} &if\ x_1\ is\ A_1^i\ and \dots and\ \ x_n\ is\ \ A_n^i\ then \\ &y^i = a_0^i + a_1^i x_1 + \dots + a_n^i x_n, \end{aligned} \tag{35}$$

In which $\mathrm{i} = 1,2,\dots,\mathrm{M}$ and M is the number of fuzzy rules. $\mathrm{y^i}$'s are the output of these M fuzzy rules and $\mathrm{a_0^i, a_1^i, \dots, a_n^i}$ are constant coefficients.

To design sliding mode controller, equation (19) could be stated as:

$$\begin{cases} F_p = \hat{F} + K - As & , \ s < 0 \\ F_n = \hat{F} - K - As & , \ s > 0, \end{cases} \tag{36}$$

With respect to equation (36), controller fuzzy rules could be stated as:

$$\begin{aligned} &if\ s\ is\ A_1^1\ and\ F_p\ is\ A_2^1\ and\ F_n\ is\ A_3^1\ \ then \\ &\quad y^1 = a_0^1 + a_1^1 s + a_2^1 u_p + a_3^1 u_n, \\ &if\ s\ is\ A_1^2\ and\ F_p\ is\ A_2^2\ and\ F_n\ is\ A_3^2\ then \\ &\quad y^2 = a_0^2 + a_1^2 s + a_2^2 u_p + a_3^2 u_n, \end{aligned} \tag{37}$$

In the aforementioned relation, $\mathrm{a_0^1 = a_0^2 = a_1^1 = a_2^2 = a_1^2 = a_3^1 = 0}$ and $\mathrm{a_2^1 = a_3^2 = 1}$ and membership functions will be defined as:

$$A_1^1 = \begin{cases} 1 & , \ s \le -\gamma_1 \\ 1 - 2(s + \gamma_1)^2 & , \ -\gamma_1 \le s \le 0 \\ 2(s - \gamma_1)^2 & , \ 0 \le s \le \gamma_1 \\ 0 & , \ s \ge \gamma_1 \end{cases}, \tag{38}$$

$$A_1^2 = \begin{cases} 0 & , \quad s \le -\gamma_2 \\ 2(s+\gamma_2)^2 & , \quad -\gamma_2 \le s \le 0 \\ 1-2(s-\gamma_2)^2 & , \quad 0 \le s \le \gamma_2 \\ 1 & , \quad s \ge \gamma_2 \quad , \end{cases} \tag{39}$$

In equations (37) and (38), γ_1 *and* γ_2 are positive constants.

$$A_2^1 = A_2^2 = 1 \quad , \quad lower\ bound\ of\ F \le F_p \le upper\ bound\ of\ F\ , \tag{40}$$

$$A_3^1 = A_3^2 = 1 \quad , \quad lower\ bound\ of\ F \le F_n \le upper\ bound\ of\ F\ , \tag{41}$$

Point 3: To design the controller for robot manipulator, designers need to have access to the information of dynamic equations of robot. In this case, the uncertainties bound of the dynamic equations of robot manipulator is determined. Therefore, for desirable performance of robot manipulator, the bound of exerted force to end-effector is determined.

Figure 1, displays the rule view window for an exemplary input.

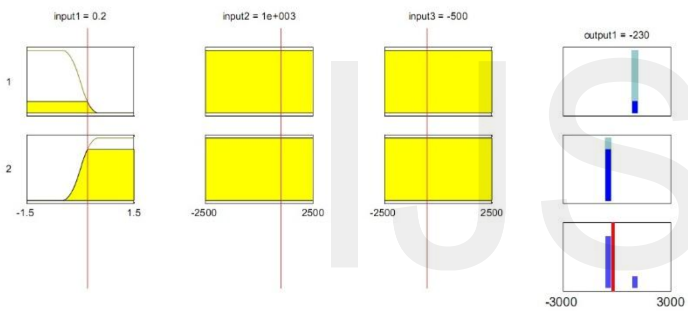

Fig. 1. Rule view of fuzzy controller for input vector of $x = [0.2, 1000, -500]^T$

Assuming $x = [s, F_p, F_n]^T$ to be input vector of fuzzy TSK system, its output will be calculated based on the combination of fuzzy rules (37) and is expressed as follows:

$$y = \frac{\sum_{i=1}^{2} f^i(x) y^i(x)}{\sum_{i=1}^{2} f^i(x)}, \tag{42}$$

$f^i(x)$ is the firing strength of the ith rule, which is obtained from the following equation:

$$f^i(x) = \mu_{A_1^i}(x_1) * \mu_{A_2^i}(x_2) * \mu_{A_3^i}(x_3)\ , \tag{43}$$

" $*$ " is the indicator of a t-norm and $\mu_{A_j^i}(x_j)$ indicates the membership degree of the input x_j in the membership function A_j^i from the ith rule. Figure 2, displays the 3D plot for the rule surface.

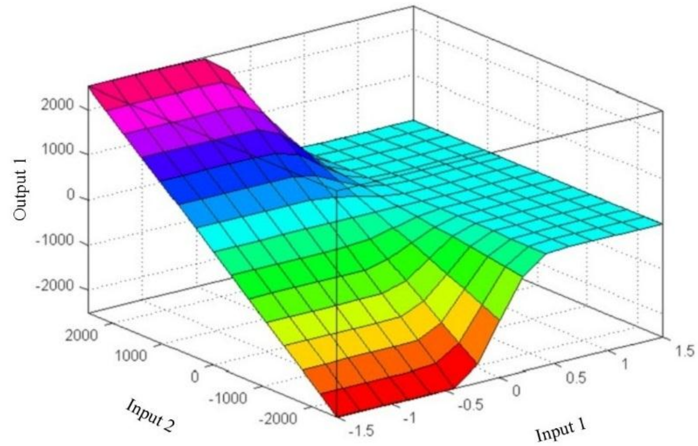

Fig. 2. The view surface for fuzzy controller

6 A CASE STUDY ON REVOLUTE DOUBLE-JOINT ROBOT MANIPULATOR

The controllers which have been designed and scrutinized in this paper are conducted on the revolute double-joint robot manipulator of figure 3.

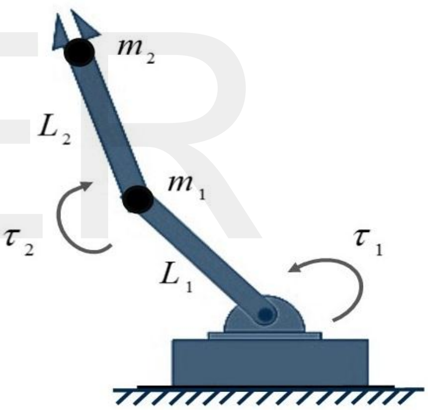

Fig. 3. Robot manipulator with two revolute joints

Dynamic equations of this robot are as follows [30]:

$$M_x(q)\ddot{X} + V_x(q,\dot{q})\dot{q} + G_x(q) + T_{dX} = F(t), \tag{44}$$

In which:

$$M_x(q) = \begin{bmatrix} m_1 + \frac{m_1}{(sinq_2)^2} & 0 \\ 0 & m_2 \end{bmatrix}, \tag{45}$$

$$V_x(q,\dot{q}) = \begin{bmatrix} V_{11} & V_{12} \\ V_{21} & V_{22} \end{bmatrix}, \tag{46}$$

$$V_{11} = -(m_2 L_1(cosq_2) + m_2 L_2)\dot{q}_1 - 2m_2 L_2 + m_2 L_1(cosq_2) + m_1 L_1 \frac{cosq_2}{(sinq_2)^2})\dot{q}_2\ , \tag{47}$$

$$V_{12} = -m_2 L_2 \dot{q}_2 \,, \tag{48}$$

$$V_{21} = m_2 L_1 (sinq_2)\dot{q}_1 + m_2 L_1 (sinq_2)\dot{q}_2 \,, \tag{49}$$

$$V_{22} = 0 \,, \tag{50}$$

$$G_x(q) = \begin{bmatrix} m_1 g \frac{cosq_1}{sinq_2} + m_2 g (sinq_1)(sinq_2) \\ m_2 g (cosq_1)(cosq_2) \end{bmatrix}, \tag{51}$$

$$T_{dx} = \begin{bmatrix} T_{d_x} \\ T_{d_y} \end{bmatrix}. \tag{52}$$

In each link, mass distribution is considered as point particle and center of mass of each link is considered to be determined at the end. L_1 represents the length of the first link, L_2 is designated as the length of the second link, m_1 is assigned as the mass of the first link, m_2 is the mass of the second link, g is the gravity, T_{dx} is the disturbance or un-modeled dynamic and F is the force exerted on the end-effector.
The quantities for the robot which are utilized in this simulation have been presented in table 1.

Point 4: $\hat{L}_1$, $\hat{m}_1$, $\hat{L}_2$, and $\hat{m}_2$ are the estimations from the actual quantities of L_1, m_1, L_2, and m_2 which have been utilized in calculation of $\hat{F}$.

TABLE 1
PARAMETERS OF REVOLUTE DOUBLE-JOINT ROBOT

L_1=1m	$\hat{L}_1$=1.1m
m_1=10kg	$\hat{m}_1$=9.5kg
L_2=0.8m	$\hat{L}_2$=0.9m
m_2=8kg	$\hat{m}_2$=7.5kg
T_{d_x}=T_{d_y}=4sin(t)	g=9.8$^m/_{s^2}$

The quantities of controlling parameters in controller (19) which have been utilized in this simulation are presented in table 2.

Point 5: Quantities k_1 and k_2 are calculated based on equation (32) and also quantities A_{11},A_{12}, $A_{21}$and A_{22} are calculated based on equation (33).

TABLE 2
CONTROLLING PARAMETERS IN ROBOT MANIPULATOR

k_1=100	k_2=200
λ_1=50	λ_2=100
A_{11} =90	$A_{12} = 0$
$A_{21} = 0$	$A_{22} = 100$
γ_1=0.5	γ_2=0.5

By the parameters mentioned in tables 1 and 2, relation (19) is applicable. Matrix $\dot{M}_x(q)$ is calculated as:

$$\dot{M}_x(q) = \begin{bmatrix} \frac{-m_1(2(sinq_2)(cosq_2))}{(sinq_2)^4} & 0 \\ 0 & 0 \end{bmatrix} = \begin{bmatrix} D_{11} & D_{12} \\ D_{21} & D_{22} \end{bmatrix}, \tag{53}$$

In equation (51), upper bound of D_{11} is specified. Thus considering Lyapunov function candidate as equation (24), we can conclude equation (30) for the robot as:

$$\dot{V}(s) = \sum_{i=1}^{2} (s_i(\Delta f_i - k_i sgn(s_i))) - s_1^2 A_{11} - s_1 s_2 A_{12} - s_2 s_1 A_{21} - s_2^2 A_{22} + \frac{1}{2} s_1^2 D_{11} \,, \tag{54}$$

To prove closed-loop system stability, equation (54) must be less than zero, that is:

$$\dot{V}(s) = \sum_{i=1}^{2} (s_i(\Delta f_i - k_i sgn(s_i))) - s_1^2 A_{11} - s_1 s_2 A_{12} - s_2 s_1 A_{21} - s_2^2 A_{22} + \frac{1}{2} s_1^2 D_{11} < 0 \,, \tag{55}$$

To satisfy the above equation, the following equations must be established:

$$K_i > \|\Delta f_i\| \quad ; \quad i = 1,2 \,, \tag{56}$$

$$\|A_{11}\| > \left\|\frac{D_{11}}{2}\right\| . \tag{57}$$

In addition, quantities of A_{12}, $A_{21}$and $A_{22}$are determined such that the matrix A to be positive-definite. Therefore, we can conclude global asymptotic stability for closed-loop system. To investigate the weaknesses of sliding mode controllers (19) and (34) and indicating the favorable operation of the proposed fuzzy sliding mode control, simulations are performed in three steps:

Step 1 of simulation: in this step, control input of equation (23) is simulated for the revolute double-joint robot.
After performing the simulation, the desired and actual trajectories in Cartesian space for end effector have been shown in figure 4.

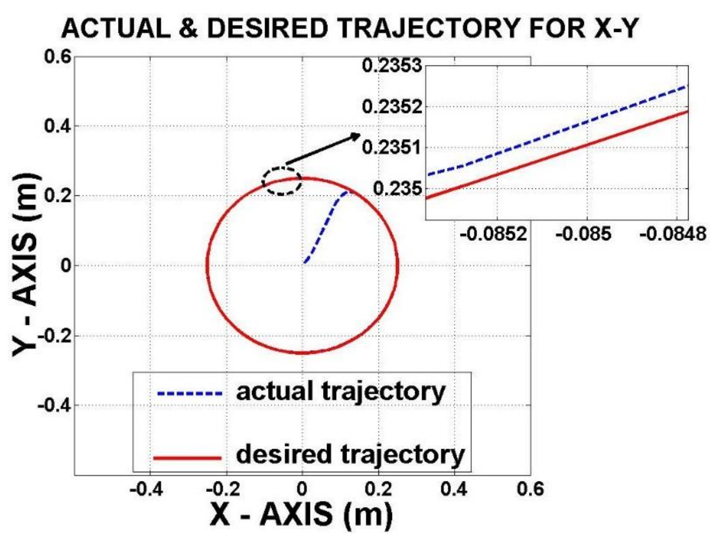

Fig. 4. The desired and actual trajectories

According to figure 4, tracking errors of the end effector position in Cartesian space for X and Y axes are shown in figure 5.

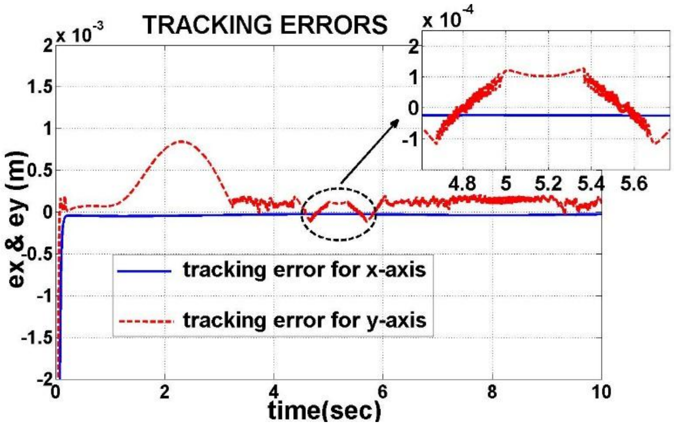

Fig. 5. Tracking error of the end effector position

As evident in figures 4 and 5, the maximum tracking error of the end-effector position is 49×10^{-6} meters for X axis and 84×10^{-5} meters for Y axis. Actual trajectory on X axis matches the desired trajectory after 0.0574 seconds. Oscillations around the zero will occur in the Y axis of tracking error of the end-effector position.

Figure 6 shows the exerted control input to the joints 1 and 2.

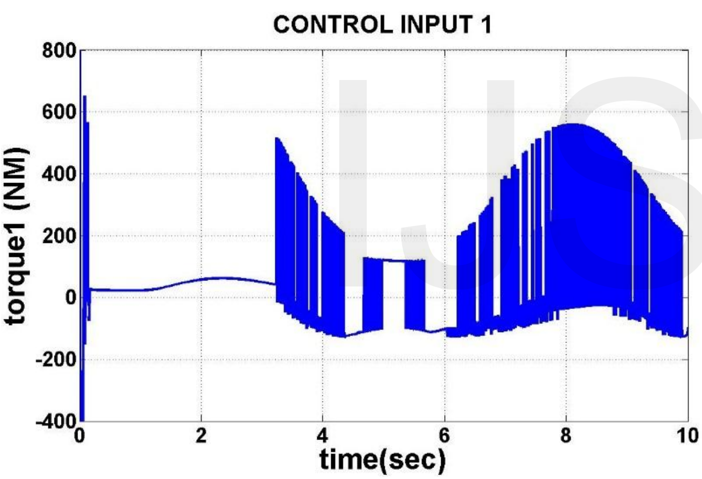

(a) The exerted control input to joint 1

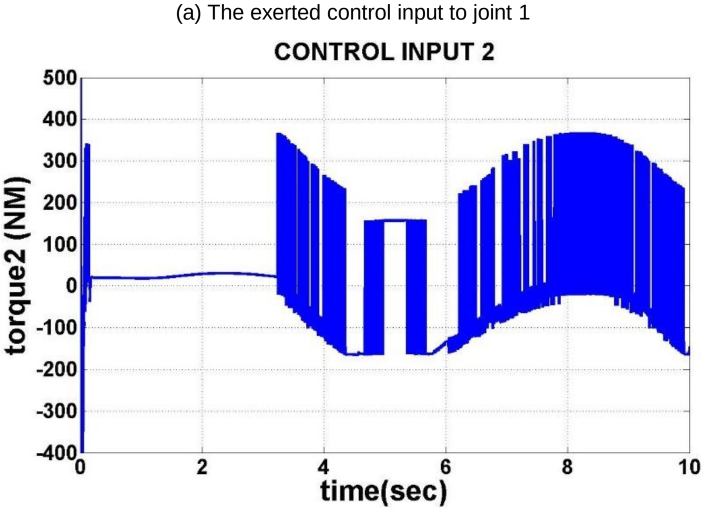

(b) The exerted control input to joint 2

Fig. 6. Exerted control inputs to joints 1 and 2

It is evident that the exerted control input has a chattering domain in the range of 225 to 700 Newton meters for joint 1 in most time intervals. This domain is from 302 to 408 Newton meters for joint 2. This chattering can lead to the activation of dynamic modes of robot manipulator.

Step 2 of simulation: To overcome the adverse chattering phenomenon in control inputs, equation (34) is simulated for revolute double-joint robot.

In this simulation, we use various quantities for ϕ_x and ϕ_y, which are demonstrated in table 3.

TABLE 3
QUANTITIES ϕ_x AND ϕ_y UTILIZED IN CONTROL EQUATION (34)

1	ϕ_x=0.75	ϕ_y=0.25
2	ϕ_x=0.15	ϕ_y=0.05
3	ϕ_x=0.003	ϕ_y =0.001

Tracking error of the end effector position on X and Y axes of Cartesian space are shown in figure 7, for various quantities of ϕ_x and ϕ_y.

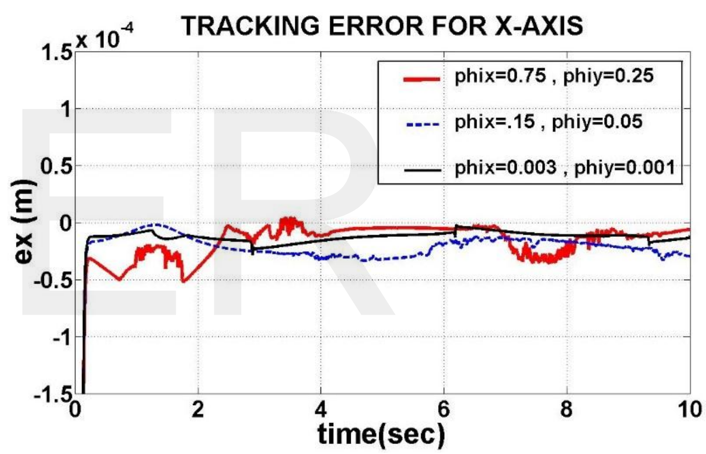

(a) Tracking error of the end effector position on X axis

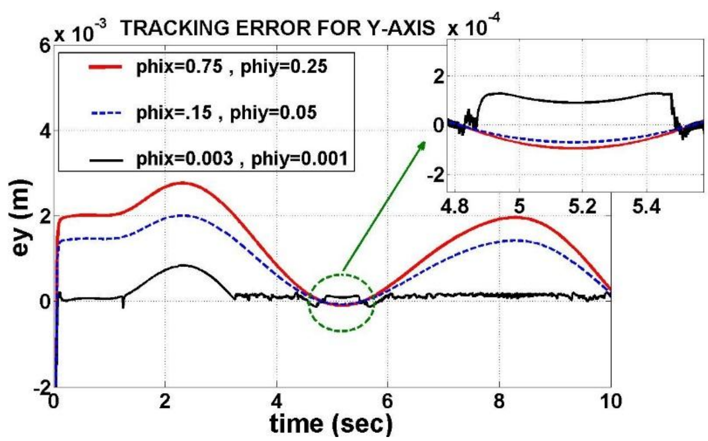

b) Tracking error of the end effector position on Y axis

Fig. 7. Tracking error on X and Y axes for various quantities of ϕ_x and ϕ_y stated in table 3

As it is shown in figure 7, the maximum tracking error occurs for larger quantities of ϕ_x and ϕ_y ; and vice versa, the minimum tracking error occurs for smaller quantities of ϕ_x and ϕ_y, such that for $\phi_x = 0.75$ and $\phi_y = 0.25$, and the maximum tracking error on X axis will be 52×10^{-6} meters. In addition, the maximum tracking error on Y axis will be 27×10^{-4} meters and although it reaches zero after 5.166 seconds, it never remains zero. For $\phi_x = 0.15$ and $\phi_y = 0.05$, the maximum tracking error on X axis will be 34×10^{-6} meters. In addition, the maximum tracking error on Y axis will be 2×10^{-3} meters. For $\phi_x = 0.0.003$ and $\phi_y = 0.001$, the maximum tracking error on X axis will be 23×10^{-6} meters, and the maximum tracking error on Y axis will be 8×10^{-4} meters after 2.295 seconds; subsequently the tracking error is very low and will be oscillated around zero till the end. Figure 8 presents the exerted control inputs to the joints 1 and 2 for $\phi_x = 0.75$, $\phi_y = 0.25$ and $\phi_x = 0.15$, $\phi_y = 0.05$.

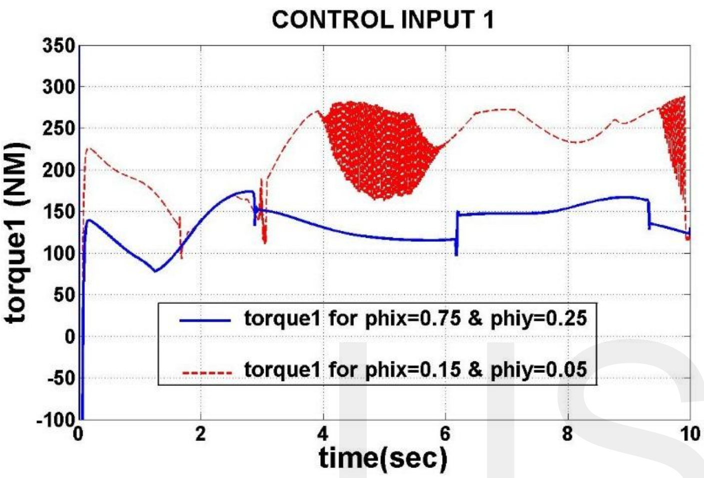

(a) Exerted control input to joint 1

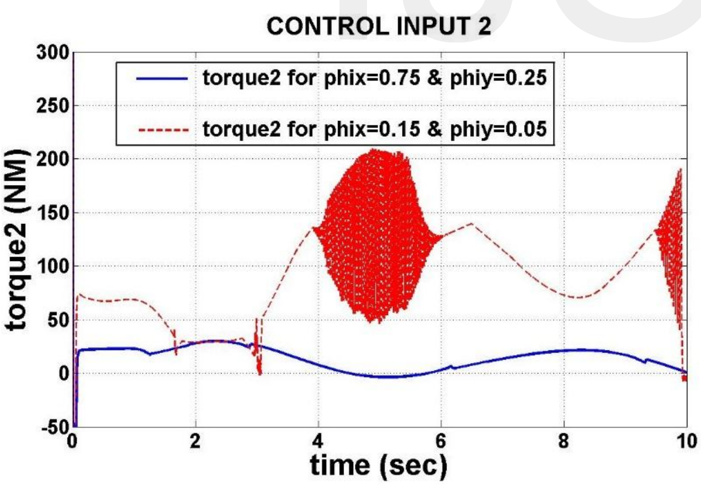

(b) Exerted control input to joint 2

Fig. 8. Exerted control inputs to joints 1 and 2 for $\phi_x = 0.75$, $\phi_y = 0.25$ and $\phi_x = 0.15$, $\phi_y = 0.05$

The increase in chattering with the reduction in quantities of ϕ_x and ϕ_y is clear from figure 8, such that for $\phi_x = 0.75$ and $\phi_y = 0.25$, control inputs have no chattering, while for $\phi_x = 0.15$ and $\phi_y = 0.05$, control input of joint 1 has a chattering domain of 98 Newton meters and that of joint 2 has a chattering domain of 160 Newton meters.

Figure 9 displays the exerted control inputs to the joints 1 and 2 for $\phi_x = 0.003$ and $\phi_y = 0.001$.

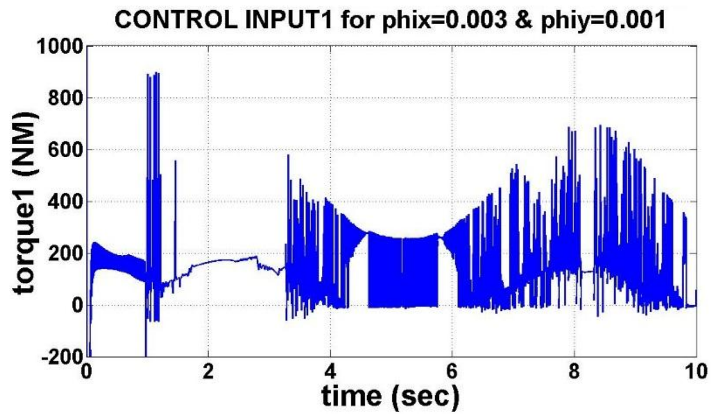

(a) Exerted control input to joint 1

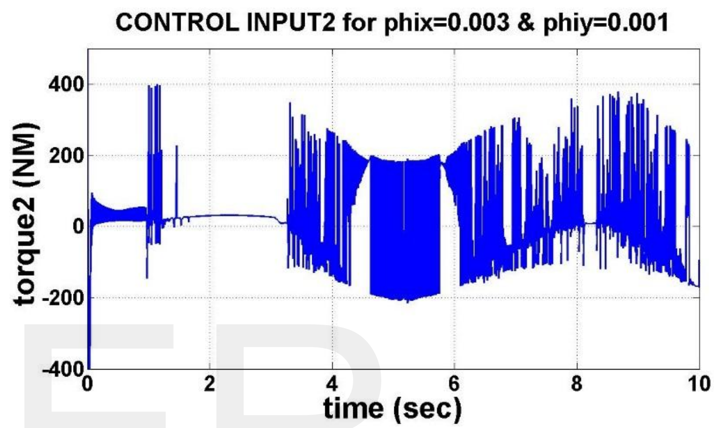

(b) Exerted control input to joint 2

Fig. 9. Exerted control inputs to joints 1 and 2 for $\phi_x = 0.003$ and $\phi_y = 0.001$

According to this figure, the chattering domain of exerted control inputs to joints 1 and 2 are 80 to 800 Newton meters and 380 Newton meters, respectively. The increase in control input chattering is clear in figure 9 compared to figure 8.

Step 3 of simulation: Fuzzy sliding mode control input is simulated for revolute double joint robot in task space.

After execution of simulation, tracking error of the end effector position on X and Y axes have been indicated in figure 10.

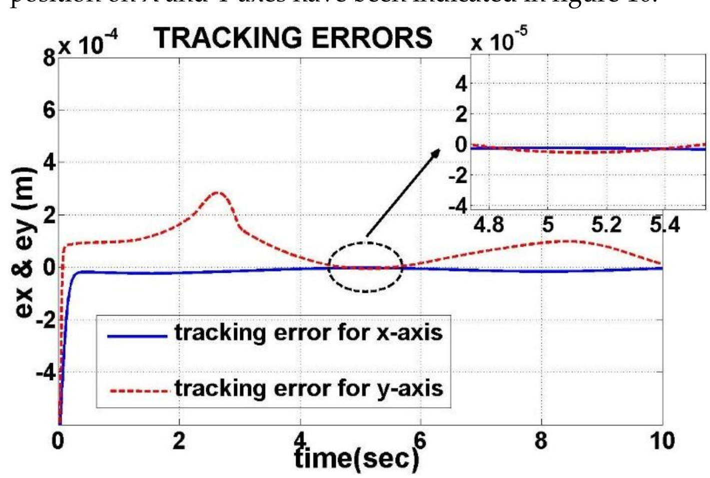

Fig. 10. Tracking error of the end effector position

According to this figure, the maximum tracking error of the end-effector position is 24×10^{-6} meters for X axis and 28×10^{-5} meters for Y axis.

Figure 11 shows control inputs for joints 1 and 2.

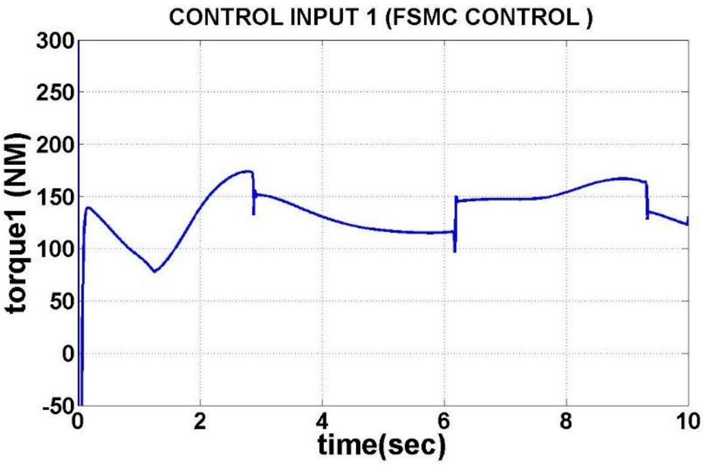

(a) Exerted control input to joint 1

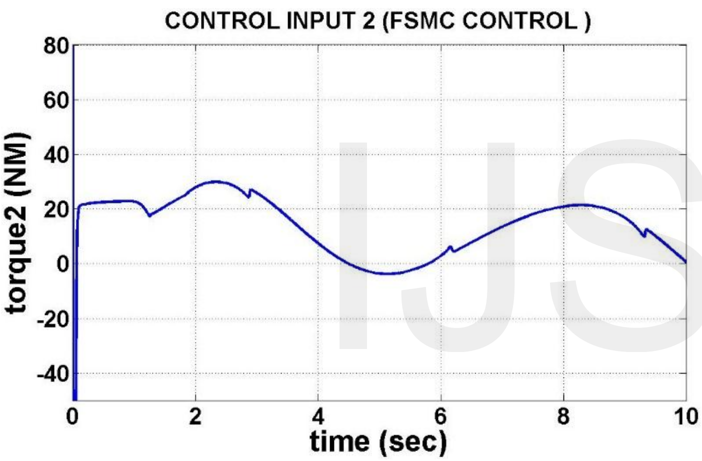

(b) Exerted control input to joint 2

Fig. 11. Exerted control inputs to joints 1 and 2

As it is understood from figure 11, control inputs for joints 1 and 2 have no chattering. Given figures 10 and 11 and comparing them with the results of previous simulations, we understand that by exerting fuzzy sliding mode control input to revolute double-joint robot, we have achieved our control objectives which were having negligible tracking error of the end-effector position close to zero and also free-of-chattering control inputs.

7 CONCLUSIONS

In this paper, a controller is designed to control the robot manipulator position in the task space. In the proposed control, the advantages of combination of feedback linearization, sliding mode control, and TSK fuzzy system are taken. In the design of the proposed controller, the following suggestions are provided:

1.The use of feedback linearization reduces the bounds of structural and non-structural uncertainties. In the proposed control, the role of feedback linearization becomes substantial when fairly accurate data on robot manipulator dynamics is available.

2.In the proposed control, the sliding mode controller is used to overcome the remaining uncertainties. In case more dynamic information on robot manipulator is available, the bounds of the remaining uncertainties are reduced. As a result, the amplitude of chattering of the control input caused by sliding mode control decreases. In case of inaccessibility to dynamic information on the robot manipulator, the bounds of the remaining uncertainties increase and, ultimately, the amplitude of the control input chattering also increases.

3.Elimination of chattering by creating a boundary layer around the sliding surface leads to tracking error in the task space.

4.The rules base of TSK fuzzy system has solely two rules. Hence, implementation of the proposed control is possible due to its low volume of calculations.

5.In the design of the TSK fuzzy system rules base, it is difficult to determine the coefficients of the rules result section, while in the proposed control, due to existence of mathematical proof in the design of the sliding mode control, the determination of the coefficients of TSK fuzzy system rules section becomes much simpler.

6.The proposed control has the ability to be optimized.

7.The results of the simulation reveals that the fuzzy sliding mode control input is free of chattering and within an allowable range in the presence of all dynamic and kinematic uncertainties in robot manipulator. Thus by using the proposed control, the concerns for robot manipulator actuators saturation are alleviated.

In addition to the aforementioned remarks, the results of the three-step simulation and the comparison of the results from the application of classic sliding mode control, the modified sliding mode control, and the fuzzy sliding mode control revealed that the performance the proposed fuzzy sliding mode control is more favorable and the tracking error of the robot manipulator in the task space in the presence of all uncertainties converges to zero.

REFERENCES

[1] Qu Z. and Dawson D. M. *Robust tracking control of robot manipulators*. IEEE Press, Inc., New York, USA, 1996.

[2] Sage H. G., De Mathelin M. F., Ostertag E. “Robust control of robot manipulators: a survey,” International Journal of Control, Vol. 72, No. 16, P. 1498–1522, 1999. doi:10.1080/002071799220137.

[3] Slotine, JJE. and Sastry S. “Tracking control of non-linear systems using sliding surfaces, with application to robot manipulators,” International journal of control, Vol.38, No.2, p. 465–492, 1983. doi:10.1080/00207178308933088.

[4] Slotine, JJE. “The robust control of robot manipulators,” The International Journal of Robotics Research, Vol. 4, No.2, p. 49–64, 1985. doi:10.1177/027836498500400205.

[5] Visioli, A., & Legnani, G. “On the trajectory tracking control of indus-

trial SCARA robot manipulators," Industrial Electronics, IEEE Transactions on, Vol. 49, No. 1, P. 224–232, 2002. doi:10.1109/41.982266.

[6] Fateh, M. M. "Nonlinear control of electrical flexible-joint robots," Nonlinear Dynamics, Vol. 67, No. 4, P. 2549-2559, 2012. doi:10.1007/s11071-011-0167-3.

[7] Fateh, M. M. "Decentralized Direct Adaptive Fuzzy Control for Flexible-Joint Robots," Journal of Control Engineering and Applied Informatics, Vol. 15, No. 4, P. 97-105, 2013.

[8] Kelly, R., Davila, V. S., & Perez, J. A. L. *Control of robot manipulators in joint space*. Springer Science & Business Media, Germany, 2006.

[9] Lewis, F. L., Dawson, D. M., & Abdallah, C. T. *Robot manipulator control: theory and practice*, Second Edition. CRC Press, USA, 2003.

[10] Nicosia, S., & Tomei, P. "Robot control by using only joint position measurements," Automatic Control, IEEE Transactions on, Vol. 35, No. 9, P. 1058-1061, 1990. doi:10.1109/9.58537.

[11] Sefriti, S., Boumhidi, J., Naoual, R., & Boumhidi, I. "Adaptive neural network sliding mode control for electrically-driven robot manipulators," Journal of Control Engineering and Applied Informatics, Vol. 14, No. 4, P. 27-32, 2012.

[12] M. Veysi and M. R. Soltanpour, "Eliminating chattering phenomenon in sliding mode control of robot manipulators in the joint space using fuzzy logic," J. Solid and Fluid Mech. Shahrood University of Technology, Vol. 2, No. 3, P. 45–54, 2012.

[13] Slotine, JJE. and Li, w. *Applied nonlinear control* (Vol. 60). Englewood Cliffs, NJ: Prentice-Hall, 1991.

[14] Utkin, V. I. *Sliding modes and their application to variable structure systems*. MIR Publisher, Moscow, 1978.

[15] Feng, Y., Yu, X., & Man, Z. "Non-singular terminal sliding mode control of rigid manipulators," Automatica, Vol. 38, No. 12, P. 2159-2167, 2002. doi:10.1016/S0005-1098(02)00147-4.

[16] Liu, J., & Wang, X. *Terminal Sliding Mode Control. In Advanced Sliding Mode Control for Mechanical Systems*, P. 137-162. Springer Berlin Heidelberg, 2011. doi:10.1007/978-3-642-20907-9_7.

[17] Brock, S. *Robust Integral Sliding Mode Tracking Control of a Servo Drives with Reference Trajectory Generator. In Analysis and Simulation of Electrical and Computer Systems*, P. 305-313. Springer International Publishing, 2015. doi:10.1007/978-3-319-11248-0_23.

[18] Fridman, L., Poznyak, A., & Bejarano, F. J. *Integral Sliding Mode Control. In Robust Output LQ Optimal Control via Integral Sliding Modes* P. 11-20. Springer New York, 2014. doi:10.1007/978-0-8176-4962-3_2.

[19] Mobayen, S. "Design of CNF-based nonlinear integral sliding surface for matched uncertain linear systems with multiple state-delays," Nonlinear Dynamics, Vol. 77, No. 3, P. 1047-1054, 2014. doi:10.1007/s11071-014-1362-9.

[20] Utkin, V., & Shi, J. "Integral sliding mode in systems operating under uncertainty conditions," In Decision and Control, Proceedings of the 35th IEEE Conference on Vol. 4, pp. 4591-4596. IEEE, 1996. doi:10.1109/CDC.1996.577594.

[21] Chen, M. S., Chen, C. H., & Yang, F. Y. "An LTR-observer-based dynamic sliding mode control for chattering reduction," Automatica, Vol. 43, No. 6, P. 1111-1116, 2007. doi:10.1016/j.automatica.2006.12.001.

[22] Koshkouei, A. J., Burnham, K. J., & Zinober, A. S. "Dynamic sliding mode control design," IEE Proceedings-Control Theory and Applications, Vol. 152, No. 4, P. 392-396, 2005. doi:10.1049/ip-cta:20055133.

[23] Boiko, I., Fridman, L., & Iriarte, R. "Analysis of chattering in continuous sliding mode control," In American Control Conference, P. 2439-2444. IEEE, 2005. doi:10.1109/ACC.2005.1470332.

[24] Defoort, M., Floquet, T., Kokosy, A., & Perruquetti, W. "A novel higher order sliding mode control scheme," Systems & Control Letters, Vol. 58, No. 2, P. 102-108, 2009. doi:10.1016/j.sysconle.2008.09.004.

[25] Levant, A. "Higher-order sliding modes, differentiation and output-feedback control," International journal of Control, Vol. 76, No. 9-10, P. 924-941, 2003. doi:10.1080/0020717031000099029.

[26] Jerouane, M., Lamnabhi-Lagarrigue, F. "Discontinuous sliding surface for a general electromechanical system with time-invariant uncertainties," In Decision and Control, European Control Conference. CDC-ECC'05. 44th IEEE Conference on P. 6800-6805. IEEE, 2005. doi:10.1109/CDC.2005.1583255.

[27] Jinggang, Z., Yibo, Z., Zhimei, C., & Zhao, Z. "A control scheme based on discrete time-varying sliding surface for position control systems," In Intelligent Control and Automation, Fifth World Congress on Vol. 2, P. 1175-1178. IEEE, 2004. doi:10.1109/WCICA.2004.1340799.

[28] Chen, C. W. "Applications of the fuzzy Lyapunov linear matrix inequality criterion to a chaotic structural system," Journal of Vibration and Control, Vol. 18, No. 13, P. 1925-1938, 2012. doi:10.1177/1077546311428346.

[29] Chiang, T. S., & Chiu, C. S. "Adaptive fast terminal sliding mode control for a class of nonlinear systems with time-varying uncertainties via LMI approach," In Systems, Man and Cybernetics. IEEE International Conference on P. 2846-2850. IEEE, 2008. doi:10.1109/ICSMC.2008.4811728.

[30] Salamanca, J. M., & Garcia, E. E. R. "Sliding mode control with linear matrix inequalities using only output information," In Industrial Electronics and Control Applications, International Conference on P. 6-15. IEEE. doi:10.1109/ICIECA.2005.1644357, 2005.

[31] Craig, J. J. *Introduction to robotics: mechanics and control* (Vol. 3). Upper Saddle River: Pearson Prentice Hall, 2005.

[32] M. Veysi, M. R. Soltanpour and M. H. Khooban, "A novel self-adaptive modified bat fuzzy sliding mode control of robot manipulator in presence of uncertainties in task space," Robotica, P. 1-20, May 2014. doi:10.1017/S0263574714001258.

[33] Khatib, O. "Dynamic control of manipulator in operational space," In Proc. 6th IFToMM World Congress on Theory of Machines and Mechanisms, P. 1128-1131, 1983.

[34] Strang, G. *Linear algebra and its applications*. Belmont, CA: Thomson, Brooks/Cole, 2006.